NASA Technical Paper 1095

Effects of Film Injection Angle on Turbine Vane Cooling

James W. Gauntner

DECEMBER 1977

NASA

NASA Technical Paper 1095

Effects of Film Injection Angle on Turbine Vane Cooling

James W. Gauntner
Lewis Research Center
Cleveland, Ohio

National Aeronautics
and Space Administration

**Scientific and Technical
Information Office**

1977

EFFECTS OF FILM INJECTION ANGLE ON TURBINE VANE COOLING

by James W. Gauntner

Lewis Research Center

SUMMARY

Film ejection from discrete holes in the suction surface of a turbine vane was studied for hole axes (1) slanted 30° to the surface in the streamwise direction and (2) slanted 30° to the surface and 45° from the streamwise direction toward the hub. The holes were near the throat area in a five-row, staggered array with 8-diameter spacing. The mass flux ratios were as high as 1.2. The data were obtained in an annular sector cascade at conditions where both the ratio of the boundary-layer-momentum-thickness-to-hole diameter and the momentum-thickness Reynolds number were typical of an advanced turbofan engine at takeoff. Wall temperatures were measured downstream of each of the rows of holes.

The data show that (1) the cooling effectiveness for compound-angle injection is greater than that of slanted in-line injection for mass flux ratios as high as 1.2; (2) the cooling effectiveness for slanted in-line injection reaches a local maximum at a mass flux ratio of about 0.5 and then decreases for greater mass flux ratios for injection into an adverse pressure gradient; and (3) the cooling effectiveness for compound-angle injection reaches a local maximum at a mass flux ratio of about 0.5 and then resumes increasing at a mass flux ratio of about 0.7. The last two results are consistent with the implications of flow visualization results of a referenced study in which film ejected from slanted in-line holes separates from the surface at a mass flux ratio of about 0.5 and film ejected from compound-angle holes remains close to the surface even at high mass-flux ratios.

Also included is a closed-form analytical solution for temperature within a film-cooled wall. The solution is subject to three homogeneous and one nonhomogeneous boundary conditions.

INTRODUCTION

Increases in turbine-inlet temperature and pressure in current and proposed aircraft have reached the point where heat-flux levels are too high to adequately cool the

hot blades of gas turbines by convection alone. Some film cooling is usually required to protect the metal parts from the hot gas stream. The most practical method currently used for film cooling aircraft turbines is to inject the cooling air into the boundary layer from discrete holes in the surface of the blades. It is important that the film be injected efficiently to provide the desired heat-transfer protection with a minimum disruption of the mainstream. Poorly designed film-injection schemes can severely reduce turbine aerodynamic efficiency and, in some instances, even increase heat transfer to the surface.

There has been considerable interest recently in discrete-hole film cooling (e. g., refs. 1 to 9). However, there is still a need for a better understanding of the fluid dynamic effects of film injection through discrete holes into a turbulent boundary layer. Colladay and Russel (ref. 10) studied some of these effects using flow visualization and presented a physical description of the interaction between an injected film and the mainstream. Their study was performed on a flat plate without a pressure gradient. Results of that study showed that if the axes of the injection holes were oriented at a compound angle to the surface and mainstream, then separation of the injected film could be delayed to higher values of the injected flow when compared with the case where the film is injected at the same angle to the surface but in the direction of the mainstream flow. Based on these results, the inference can be made that compound-angle film injection would offer better thermal protection to the surface at higher mass-flux ratios than in-line film injection.

The purpose of this study is to verify the improved cooling effectiveness of compound injection relative to in-line injection as inferred from the flow visualization results and to explore the design implications which these heat-transfer results have on the film cooling of turbine vanes.

Tests were conducted in an annular sector cascade at conditions that simulated the environment in the turbine of an advanced turbofan engine. The environments simulated included gas pressures as high as 38 atmospheres and gas temperatures as high as 1700 K. To simulate the turbine environments, the vanes had the same momentum-thickness Reynolds number, Mach number, and ratio of momentum thickness to hole diameter (ref. 11). Film injection from discrete holes was studied for hole axes (1) slanted 30° to the surface in the direction of the mainstream and (2) slanted 30° to the surface and 45° laterally to the mainstream toward the hub. These holes were in the suction surface of a turbine vane near the throat area in a five-row staggered array. Both the row-to-row spacing and the hole-to-hole spacing within a row were 8 diameters. The coolant-to-gas mass flux ratios were as high as 1.2.

Results of this study are expressed as a comparison of cooling effectiveness of the in-line angle injection and the compound-angle injection as a function of mass-flux

ratio. These results are compared with inferences from flow visualization results from reference 10.

SYMBOLS

C	constant
h	heat-transfer coefficient
k	thermal conductivity
L	one-half of distance between adjacent film-cooling holes
M	mass-flux ratio, $(\rho V)_c/(\rho V)_g$
P	turbine-inlet pressure
R	gas constant
T	temperature
t	thickness of copper strip
V	velocity
X	functional dependence of temperature within copper strip in spanwise direction
x	spanwise coordinate within copper strip as defined in fig. 7
Y	functional dependence of temperature within copper strip normal to surface
y	normal coordinate within copper strip as defined in fig. 7
α	$\pi t/L$
Γ	function of γ as defined by eq. (2)
γ	specific heat ratio
θ	local temperature of copper strip referenced to average ambient temperature
λ	separation constant for eq. (A13)
μ	viscosity
ρ	density
φ	cooling effectiveness, $(T_g - T_w)/(T_g - T_c)$

Subscripts:

av	average
c	coolant

e	engine
g	hot gas
m	m^{th} term in series
max	maximum
n	n^{th} term in series
t	test condition
w	wall
∞	ambient

APPARATUS

Cascade Description

The cascade test facility was designed to operate at average inlet-gas temperatures as high as 1645 K and pressures up to 10 atmospheres. The facility consists of five basic components: (1) an inlet section, (2) a combustor section, (3) a transition section, (4) a test section, and (5) an exhaust section.

The test section is a 23° annular sector of a vane row and contained four vanes and five flow channels. A cross-sectional view of the cascade facility is shown in figure 1(a) and a plan view of the test section is shown in figure 1(b). The central flow channel was formed by the suction surface of vane 2 and the pressure surface of vane 3. The two outer vanes completed the flow channels for the two central vanes and also served as radiation shields between these vanes and the water-cooled cascade walls. Each test vane (vanes 2 and 3) had its own cooling-air system, which was metered by a venturi. A more detailed description of this facility is given in reference 12.

Vane Description

A J-75 size vane with a span of 9.78 centimeters and a chord of 6.28 centimeters was used in this investigation. The vane material was Udimet 700. All of the cooling air entered through the vane tip plenum and issued through the film-cooling holes. The leading-edge and trailing-edge regions were solid and therefore uncooled.

Seventy-three 0.038-centimeter-diameter holes were electrical-discharge machined into the suction surface of each of the two vanes. Vane 3 (fig. 1(b)) had in-line angle holes and vane 2 had compound-angle holes. The axes of the in-line holes were angled at 30° to the surface and parallel to the plane of the endwall. The axes of the compound-angle holes were angled at 30° to the surface and 45° from the streamwise

direction toward the hub of the vane.

The holes were arranged in five, spanwise rows in a staggered array. Row-to-row and hole-to-hole spacing within a row was 8 hole diameters (0.30 cm). Fifteen holes were in spanwise rows 1, 3, and 5, and 14 holes were in rows 2 and 4.

INSTRUMENTATION

Figure 2 is a photograph of the four-vane cascade, looking upstream. Test vane 2 with the compound hole angles and test vane 3 with the in-line hole angles are shown in the figure. Notice the copper strips downstream of each of the five rows of holes on the two test vanes. These copper strips were used to obtain average surface temperatures by means of a closed ball Chromel/Alumel thermocouple embedded within and soldered to the strip. Calculations have shown that the difference between the measured temperature and the average surface temperature attributable to the uncertainty in the location of the thermocouple junction is less than 0.12 K. (See the appendix for a closed-form, analytical solution for the temperature distribution within the copper strip.)

The copper strip and thermocouple constitute the thermocouple assembly, the details of which are shown in figure 3. Each strip was 0.043 centimeter thick by 0.076 centimeter wide by about 2.5 centimeter long and was insulated from the test vane by means of a 0.005-centimeter-thick calcia-stabilized zirconia coating. Details of the coating can be found in reference 13. The thermal conductivity of the coating is 3.3 percent of the vane material, Udimet 700, and 0.2 percent of the copper strip. These insulated copper strips with the embedded thermocouples were then placed in slots and bonded to the vane. Notice in figure 3 that the depth and width of the copper strips were limited in size by the nearness of the upstream and downstream edges of the adjacent rows of holes.

Solid vanes instrumented with pressure taps were located in positions 2 and 3 as shown in figure 1(b) and used to obtain a surface static-pressure distribution.

TEST PROCEDURE

Before the installation of the film-cooled test vanes, the solid vanes with the pressure taps were installed in the four-vane cascade. The hot-gas flow was adjusted so that the local flow in the vicinity of the throat area was barely subsonic. The resulting Mach-number distribution on the vane surface was used during the heat-transfer testing.

Equation (1) (eq. (5) of ref. 11) gives the functional relation between gas pressure

and temperature for similarity between test and engine conditions, which provides the same Reynolds number, momentum thickness, and critical-Mach-number distributions around the vane.

$$\left(\frac{P_g}{\mu_g}\frac{\Gamma_g}{\sqrt{RT_g}}\right)_t = \left(\frac{P_g}{\mu_g}\frac{\Gamma_g}{\sqrt{RT_g}}\right)_e \tag{1}$$

where

$$\Gamma_g = \sqrt{\gamma}\left(\frac{2}{\gamma+1}\right)^{(\gamma+1)/[2(\gamma-1)]} \tag{2}$$

Figure 4 displays the functional relation of equation (1) for an advanced turbofan and the corresponding test conditions of this report. At takeoff the engine was assumed to have a turbine-inlet pressure of 38 atmospheres and a turbine-inlet temperature of 1700 K; the same engine at cruise had a turbine-inlet pressure of 8.5 atmospheres and a turbine-inlet temperature of 1600 K. The maximum gas pressure of the test facility required relatively low gas temperatures to simulate the engine conditions. The resulting low gas temperatures were also compatible with the materials used in the construction of the thermocouple assemblies. (See fig. 4.) The test conditions are listed in table I.

Simulation of coolant conditions between an engine and a test requires that the ratio T_g/T_c be duplicated. Rather than modify the facility to provide the required low-temperature cooling air, a decision was made to use ambient temperature cooling air and permit departure from exact similitude. Because T_g/T_c is lower than that needed for exact similitude, the coolart-flow to gas-stream-momentum ratio is higher for a given mass-flux ratio. So the injected flow will penetrate further into the gas stream. This, however, will occur for both injection methods. As a consequence, measured values of cooling effectiveness permit a valid comparison of the relative performance of the two injection methods.

Because T_g/T_c is not maintained between test and engine conditions, T_g/T_w is not maintained. This would affect the momentum thickness and the momentum-thickness Reynolds number, but reference 10 shows these parameters to be insensitive to T_g/T_w on the suction surface near the throat region.

For each data set the mass-flux ratio was varied from 0 to 1.2. For all testing the mainstream flow was set so as to maintain an inlet Mach number of 0.24 to the vane row. As a result the local gas velocity in the throat region on the suction-surface midspan was slightly subsonic (the Mach number was about 0.98).

The mass-flux ratio for each row of holes was obtained by dividing the coolant flux by the gas flux. The coolant flux was calculated using the measured total coolant flow divided by the flow area of all five rows. The gas flux was calculated using the static-to-total gas pressure ratio measured near the center of the five-row array. This assumed a uniform mass-flux ratio over the entire array.

RESULTS AND DISCUSSION

Film ejection from discrete holes near the throat region in the suction surface of a turbine vane was studied for two hole configurations. Reference 10 performed a similar study using flow visualization. Because these studies reinforce each other, flow-visualization results of reference 10 are herein compared with the heat-transfer results of the present study.

The heat-transfer performances for in-line and compound injections were measured for both the cruise and takeoff environments of an advanced turbofan. The results for the two environments are similar, so that only the data for the takeoff conditions are presented.

Pressure Distribution

Figure 5 presents the dimensionless static-pressure distribution around the airfoils. Note the locations of the film-injection holes relative to the existing pressure gradient. The upstream row of holes, station 1, injects into a slightly favorable pressure gradient; station 3 injects into a nearly zero pressure gradient, and the last row, station 5, injects into an adverse pressure gradient. The Mach number calculated in the region of the film cooling holes, using the measured pressure ratio, is about 0.98.

Heat Transfer

Figure 6 presents a comparison of cooling effectiveness data between the slanted in-line injection and the compound-angle injection. The data in figure 6 are from stations 1 to 5, as shown in figures 2 and 5. Figure 6 shows the cooling effectiveness $[\varphi = (T_g - T_w)/(T_g - T_c)]$ for compound-angle injection to be greater than that of slanted in-line injection for mass-flux ratios up to 1.2.

Slanted in-line injection. - As shown in figure 6, for slanted in-line injection φ reaches a local maximum at a mass flux ratio M of 0.5. This phenomenon is consistent both with the flat plate, zero pressure gradient heat-transfer data in the literature and with what was inferred from the flow visualization data of reference 10. In refer-

ence 10 the injected film begins to separate from the surface at $M = 0.5$, allowing the mainstream to wrap around and under the jets. Thus a decrease in cooling effectiveness at $M > 0.5$ can be inferred from the flow-visualization tests. The local maximum in the value of φ was observed to occur at $M = 0.5$ for all measuring locations on the vane, regardless of the pressure gradient into which the film is injected.

For injection into a zero or adverse pressure gradient (stations 3 to 5), φ decreases as M increases from 0.5 to 1.2. As before, this phenomenon is consistent with both other heat-transfer data and the inferences from the flow-visualization data. According to the flow visualization results, at $M = 0.8$, the film has separated from the surface, and at $M = 1.4$ the film has penetrated into the free stream. However, for injection into a slightly favorable pressure gradient (stations 1 and 2), φ increases after undergoing a local minimum at about $M = 0.6$.

Compound-angle injection. - The cooling effectiveness of compound-angle injection does not seem to be as strongly influenced by the mainstream pressure gradient as does that of the in-line injection. As shown in figure 6 for compound-angle injection, φ reaches a local maximum at a $M = 0.5$ and then decreases slightly. At $M = 0.7$ φ begins to increase at all thermocouple stations shown in figure 6 regardless of the pressure gradient. The flow visualization results showed that the film remained close to the surface for the compound-angle injection due to a strong vortex motion. Thus a nondecreasing cooling effectiveness can be inferred from the flow visualization tests. This inference is consistent with the cooling effectiveness data in figure 6.

The minimum appearing in figure 6 can be explained by another phenomena described in reference 10. The vortex motion associated with compound-angle injection began to form at about $M = 0.3$ and became most pronounced at M's between 0.7 and 0.9. The minimum in the cooling effectiveness could be caused by a maximum in the gas-side heat-transfer coefficient resulting from the turbulence produced by the pronounced vortex motion.

CONCLUDING REMARKS

The comparison of the two injection methods shows the cooling superiority of the compound-injection angle over in-line injection when applied near the throat region on the suction surface of a turbine vane. The compound injection had a higher φ at all ratios investigated to an M of 1.2. As can be seen in figure 6, the benefits become increasingly greater at higher values of M and also as the pressure gradient becomes more adverse (fig. 6(d) and (e)).

These results show that departure of the cooling film from the surface can apparently be delayed to higher values of mass flux ratio if the film-cooling holes are

oriented at a compound angle to the surface and mainstream. This use of compound-angle holes would be especially effective in local areas on the turbine blade where the boundary layer has a tendency to separate such as in the diffusion region on the convex side of the blade or where high mass-flux ratios cannot be avoided.

On other areas of the vane surface, additional heat-transfer tests are needed to determine whether in-line or compound injection gives higher cooling effectiveness. The results of an aerodynamic investigation of a full film-cooled vane are reported in reference 14. This reference shows that, for a given coolant flow, compound-angle injection results in somewhat poorer thermodynamic efficiency than in-line injection over the entire vane surface. However, if compound angle injection is found to give higher cooling effectiveness than in-line injection, then the compound-angle holes would require less coolant flow than the in-line angle holes. Since thermodynamic efficiency generally improves with reduced coolant flow, the vane with compound angle injection might have better thermodynamic efficiency than those with in-line injection.

SUMMARY OF RESULTS

Film injection from discrete holes in the suction surface of a turbine vane was studied for (1) in-line hole angles slanted 30° to the surface in the streamwise direction and (2) compound hole angles slanted 30° to the surface and 45° from the streamwise direction toward the vane hub. The holes were near the throat area in a five-row staggered array with 8-diameter spacing. The results are as follows:

1. The cooling effectiveness for compound angle injection is greater than that of slanted in-line injection for mass flux ratios up to 1.2.

2. For compound-angle injection the cooling effectiveness resumes increasing at a mass-flux ratio of 0.7 regardless of the mainstream pressure gradient.

3. For slanted, in-line injection the cooling effectiveness reaches a local maximum at a mass flux ratio of 0.5. For a mainstream zero or adverse pressure gradient, the cooling effectiveness continues to decrease with increasing mass-flux ratios greater than 0.5. For slightly favorable pressure gradients the cooling effectiveness resumes increasing at a mass flux ratio of about 0.6.

4. The cooling effectiveness data substantiate the results inferred from a flow visualization study of the interaction of a mainstream and an injected film. The observed strong vortex motion given to the injected film by the compound-angle holes keeps the boundary layer close to the surface even at high mass-flux ratios, thereby maintaining high cooling effectiveness. The observed separation of the boundary layer

from the surface at mass-flux ratios above 0.5 with the in-line holes accounts for the decrease in cooling effectiveness.

Lewis Research Center,
National Aeronautics and Space Administration,
Cleveland, Ohio, August 12, 1977,
505-04.

APPENDIX - ANALYTICAL TEMPERATURES WITHIN A FILM-COOLED WALL

A copper strip was inserted into the surface of a turbine vane downstream of a row of film cooling holes; it was insulated from the vane by means of a calcia stabilized zirconia coating. The purpose of the copper strip was to average the cooling effect of the ejected film. The insulation reduced the influence of convection and conduction cooling from the vane interior and isolated the strip from heat conduction from adjacent rows of film-cooling holes. This cooling effect was measured by means of a thermocouple embedded within and soldered to the copper strip. It was considered important to know whether the location of the thermocouple junction relative to the location of the film-cooling holes had a significant effect on providing an accurate measurement of the average surface temperature of the copper strip.

The heat-transfer process was modeled by two-dimensional conduction, that is, both normal to the vane surface and along the span of the vane. As shown in figure 7 this plane is bounded by (1) two spanwise-adjacent film-cooling holes, (2) the copper-hot gas interface, and (3) the copper-zirconia interface. Conduction in the chordwise direction was neglected because the chordwise dimension was small compared with the spanwise dimension.

The physics of the problem yield the following partial differential equation and boundary conditions:

$$\frac{\partial^2 T(x, y)}{\partial x^2} + \frac{\partial^2 T(x, y)}{\partial y^2} = 0 \tag{A1}$$

$$\left.\frac{\partial T}{\partial x}\right|_{x=L} = 0 \qquad \text{by symmetry} \tag{A2}$$

$$\left.\frac{\partial T}{\partial x}\right|_{x=0} = 0 \qquad \text{by symmetry} \tag{A3}$$

$$\left.\frac{\partial T}{\partial y}\right|_{y=0} = 0 \qquad \text{by assuming an adiabatic surface} \tag{A4}$$

$$h[T(x, t) - T_\infty(x)] = -k \left.\frac{\partial T}{\partial y}\right|_{y=t} \tag{A5}$$

where

$$T_\infty(x) = T_{\infty,\,av} + (T_{\infty,\,max} - T_{\infty,\,av})\cos\left(\frac{\pi x}{L}\right)$$

as shown in figure 7. The method of solution is outlined as follows:

(1) Define the dependent variable as

$$\theta(x, y) = T(x, y) - T_{\infty,\,av} \tag{A6}$$

and

$$\theta_o = T_{\infty,\,max} - T_{\infty,\,av}$$

(2) Express the governing equation and boundary conditions in terms of $\theta(x, y)$

$$\frac{\partial^2\theta(x, y)}{\partial x^2} + \frac{\partial^2\theta(x, y)}{\partial y^2} = 0 \tag{A7}$$

$$\left.\frac{\partial\theta}{\theta x}\right|_{x=L} = 0 \qquad \text{by symmetry} \tag{A8}$$

$$\left.\frac{\partial\theta}{\partial x}\right|_{x=0} = 0 \qquad \text{by symmetry} \tag{A9}$$

$$\left.\frac{\partial\theta}{\partial y}\right|_{y=0} = 0 \qquad \text{by assuming an adiabatic surface} \tag{A10}$$

$$h\left[\theta(x, t) - \theta_o \cos\left(\frac{\pi x}{L}\right)\right] = -k\left.\frac{\partial\theta}{\partial y}\right|_{y=t} \tag{A11}$$

(3) Use a Separation of Variables solution;

$$\theta(x, y) = X(x)Y(y) \tag{A12}$$

insert equation (A12) into equation (A7) to obtain (A13); and choose the separation constant such that the x direction is the homogeneous direction.

$$\frac{1}{X}\frac{d^2X(x)}{dx^2} = -\frac{1}{Y}\frac{d^2Y(y)}{dy^2} = -\lambda^2 \tag{A13}$$

(4) The following solution results after applying boundary conditions (A8) to (A10):

$$\theta(x, y) = \sum_{n=0}^{\infty} C_n \cos(\lambda_n x)\cosh(\lambda_n y) \tag{A14}$$

where

$$\lambda_n = \frac{n\pi}{L} \qquad n = 0,\ 1,\ 2,\ \ldots$$

(5) The infinite number of constants C_n are evaluated by inserting equation (A14) into equation (A11), which is the remaining boundary condition, multiplying each side of the resulting equation by $\cos(\lambda_m x)$, and integrating over x from 0 to L. As a result of these actions,

$$C_1 = \frac{\theta_o}{\cosh\left(\frac{\pi t}{L}\right) + \frac{k\pi}{hL}\sinh\left(\frac{\pi t}{L}\right)} \qquad C_n = 0,\ n \neq 1 \tag{A15}$$

(6) If we define $\alpha = \pi t/L$ and insert equation (A15) into equation (A14) the following solution results:

$$\frac{\theta}{\theta_o} = \frac{\cos\left(\frac{\pi x}{L}\right)\cosh\left(\frac{\pi y}{L}\right)}{\cos\alpha + \left(\frac{k\pi}{hL}\right)\sinh\alpha} \tag{A16}$$

or using the definitions of θ and θ_o,

$$\frac{T(x, y) - T_{\infty, av}}{T_{\infty, max} - T_{\infty, av}} = \frac{\cos\left(\frac{\pi x}{L}\right)\cosh\left(\frac{\pi y}{L}\right)}{\cosh\alpha + \left(\frac{k\pi}{hL}\right)\sinh\alpha} \tag{A17}$$

A normalized temperature distribution within the copper strip obtained from equation (A17) appears in figure 8 and also below as equation (A18).

$$\frac{T(x, y) - T(L, t)}{T(0, t) - T(L, t)} = \frac{1}{2}\left[1 + \cos\left(\frac{\pi x}{L}\right)\frac{\cosh\left(\frac{\pi y}{L}\right)}{\cosh\left(\frac{\pi t}{L}\right)}\right] \tag{A18}$$

Note in the figure that the isotherms are normal to three of the four boundaries, which is consistent with boundary conditions (A2) to (A4). Also, the normalized temperature equals zero at the point of film ejection and equals unity at the point between adjacent film-cooling holes.

The junction of the thermocouple was accurately located in the y direction at a distance t/4 from the base of the copper strip. However, the location of the junction in the x direction relative to the locations of the film-cooling holes was less certain. As a result a question existed as to how well the measured temperature represented the average surface temperature. From figure 8 the dimensionless surface temperature is observed to be symmetrical about 0.5. Therefore, the average dimensionless temperature is 0.5, while the measured dimensionless temperature could be as high as 0.86 or as low as 0.14, for an uncertainty of ±0.36.

To convert from a dimensionless temperature difference of ±0.36 to an actual temperature difference, equation (A18) must be multiplied by the quantity $[T(0, t) - T(L, t)]$. By evaluating equation (A17) at $y = t$ and converting it into a temperature difference between $x = 0$ and $x = L$, the following equation can be obtained:

$$T(0, t) - T(L, t) = \frac{2(T_{\infty, \max} - T_{\infty, av})}{1 + \left(\frac{k\alpha}{ht}\right)\tanh(\alpha)} \tag{A19}$$

To obtain the actual surface temperature difference indicated in equation (A19) assumptions must be made for values of the maximum and average gas temperatures as well as the heat-transfer coefficient. Using typical values for the test conditions of $(T_{\infty, \max} - T_{\infty, av}) = [T_g - (T_g + T_c)/2] = 36$ K and $h = 9 \times 10^6$ J/(hr-m^2-K), the maximum wall surface temperature difference between holes was 0.32 K. Therefore, the maximum possible error between the average surface temperature and the measured wall temperature is ±0.12 K, that is, (0.32 K) (±0.36).

REFERENCES

1. Eriksen, V. L.: Film Cooling Effectiveness and Heat Transfer With Injection Through Holes. (HTL-TR-102, Minn. Univ.; NASA Contract NAS3-13200.) NASA CR-72991, 1971.

2. Liess, Christian: Film Cooling With Ejection From a Row of Inclined Circular Holes - An Experimental Study for the Application to Gas Turbine Blades. VKI-TN-97, von Karman Inst. for Fluid Dynamics, (Belgium), 1973.

3. Choe, H.; Kays, W. M.; and Moffat, R. J.: The Superposition Approach to Film Cooling. ASME Paper 74-WA/HT-27, Nov. 1974.

4. Choe, H.; Kays, W. M.; and Moffat, R. J.: The Turbulent Boundary Layer on a Full-Coverage Film-Cooled Surface - An Experimental Heat Transfer Study With Normal Injection. NASA CR-2642, 1976.

5. Crawford, M. E.; et al.: Full-Coverage Film Cooling Heat Transfer Study - A Summary of the Data for Normal-Hole Injection and 30° Slant-Hole Injection. NASA CR-2648, 1976.

6. Metzger, D. E.; Takeuchi, D. I.; and Kuenstler, P. A.: Effectiveness and Heat Transfer With Full-Coverage Film Cooling. J. Eng. Power, vol. 95, no. 3, July 1973, pp. 180-184.

7. Mayle, R. E.; and Camarata, F. J.: Multihole Cooling Film Effectiveness and Heat Transfer. J. Heat Transfer, vol. 97, no. 4, Nov. 1975, pp. 534-538.

8. LeBrocq, P. V.; Launder, B. E.; and Priddin, C. H.: Discrete Hole Injection as a Means of Transpiration Cooling; An Experimental Study. Inst. Mech. Eng. (London) Proc., vol. 187, no. 17, 1973, pp. 149-157.

9. Launder, B. E.; and York, J.: Discrete Hole Cooling in the Presence of Free Stream Turbulence and a Strong Favourable Pressure Gradient. HTS/73/9, Coll. Sci. Technol. (London), 1973.

10. Colladay, R. S.; and Russell, L. M.: Streamline Flow Visualization of Discrete Hole Film Cooling for Gas Turbine Applications. J. Heat Transfer, vol. 98, no. 2, May 1976.

11. Colladay, Raymond S.; and Stepka, Francis S.: Similarity Constraints in Testing of Cooled Engine Parts. NASA TN D-7707, 1974.

12. Calvert, Howard F.; et al.: Turbine Cooling Research Facility. NASA TM X-1927, 1970.

13. Liebert, Curt H.; and Stepka, Francis S.: Ceramic Thermal-Barrier Coatings for Cooled Turbines. NASA TM X-73426, 1976. (Also AIAA Paper 76-729, July 1976.)

14. Moffitt, Thomas P.; Stepka, Francis S.; and Rohlik, Harold E.: Summary of NASA Aerodynamic and Heat Transfer Studies in Turbine Vanes and Blades. NASA TM X-73518, 1976.

TABLE I. - ENGINE AND TEST CONDITIONS

FOR AN ADVANCED TURBOFAN

Condition	Takeoff	Cruise
Engine conditions:		
Combustor exit temperature, K	1700	1600
Combustor exit pressure, atm	38.0	8.5
Cooling air temperature, K	873	502
Test conditions:		
Combustor exit temperature, K	367	478
Combustor exit pressure, atm	6.15	2.04
Cooling air temperature, K	300	300
Momentum thickness Reynolds number	2942	772
Ratio of boundary layer thickness to hole diameter	1.19	1.31

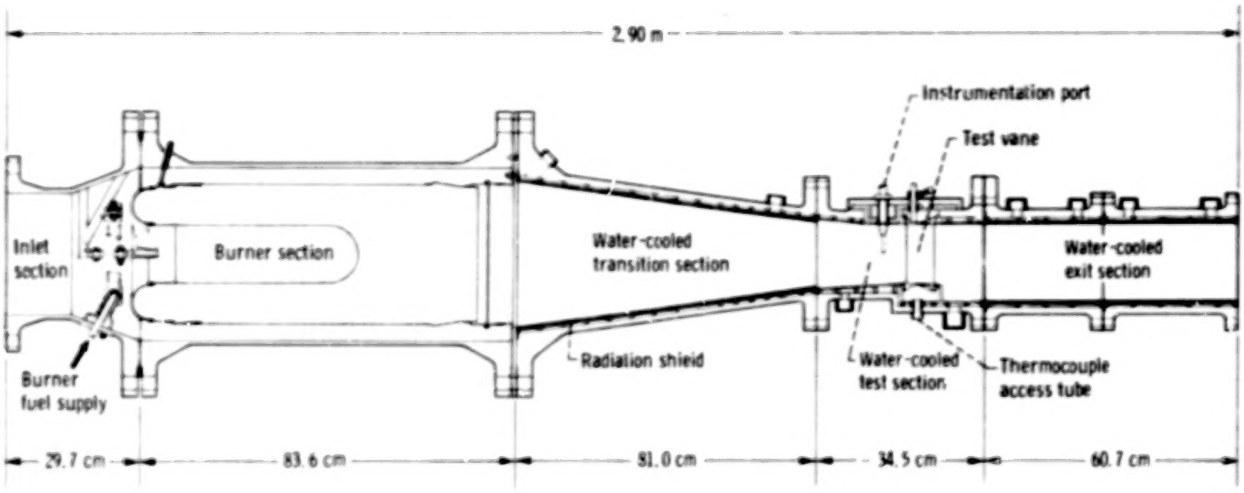

(a) Cascade facility.

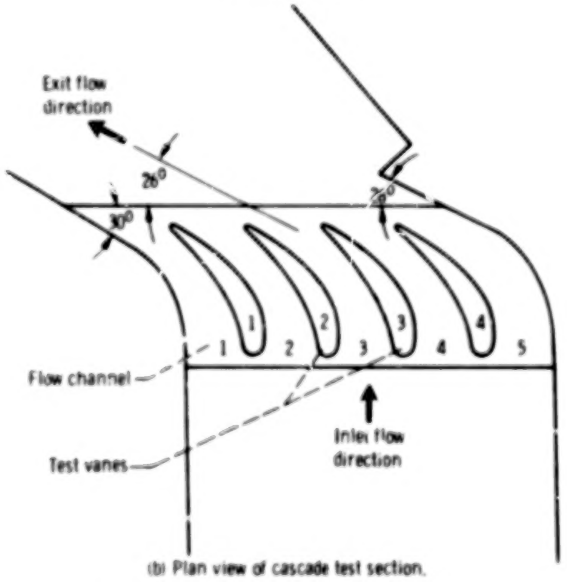

(b) Plan view of cascade test section.

Figure 1. - Schematic of cascade test section.

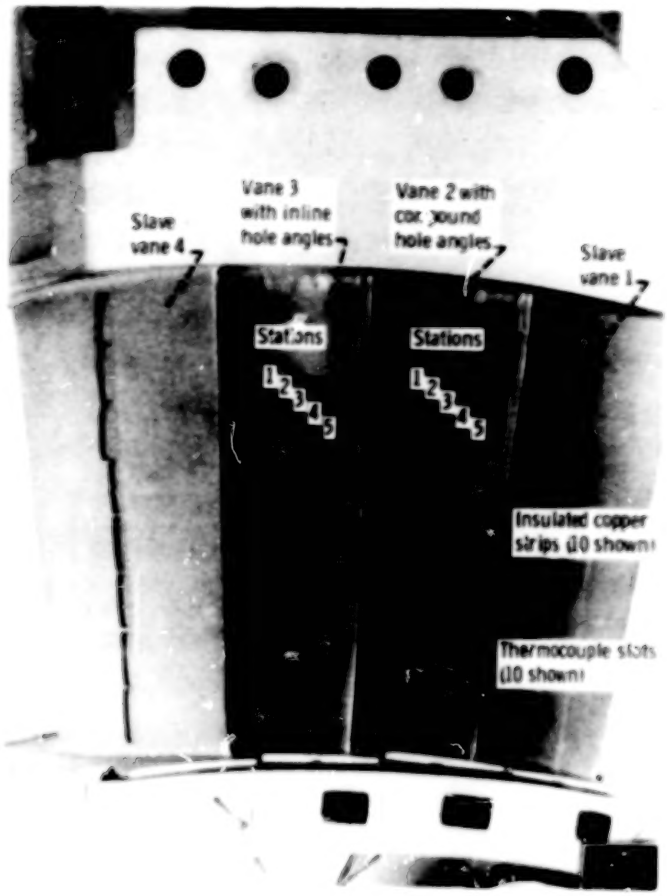

Figure 2. - Four-vane cascade with location of insulated copper strips on test vanes shown.

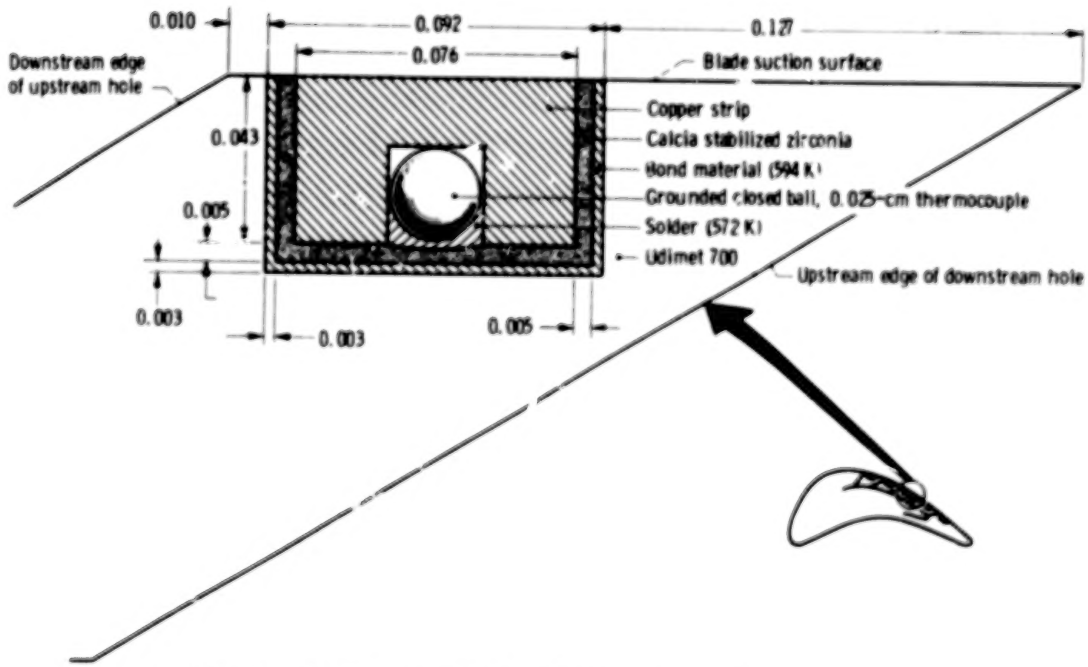

Figure 3. - Details of location and installation of thermocouple assembly. (All dimensions are in cm.)

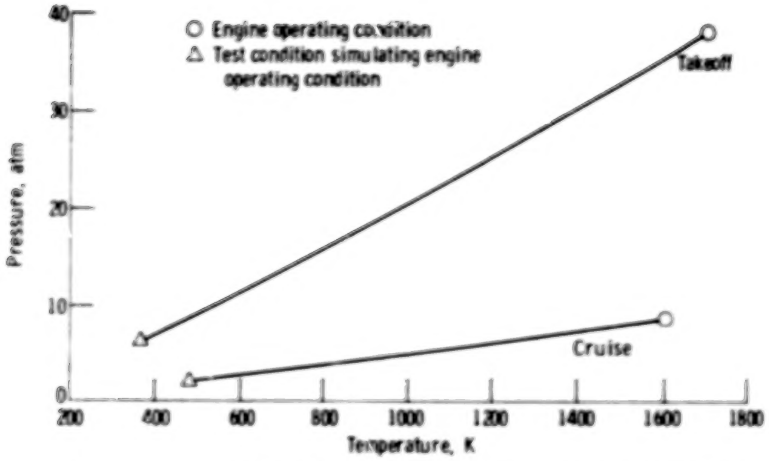

Figure 4. - Similarity curves for combustion-gas environments of advanced turbofan engine at takeoff and at cruise.

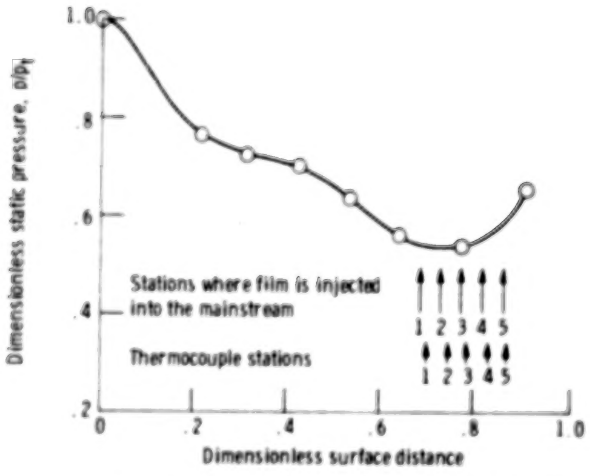

Figure 5. - Experimental midspan distribution of vane suction-surface pressure ratios obtained from cascade tests.

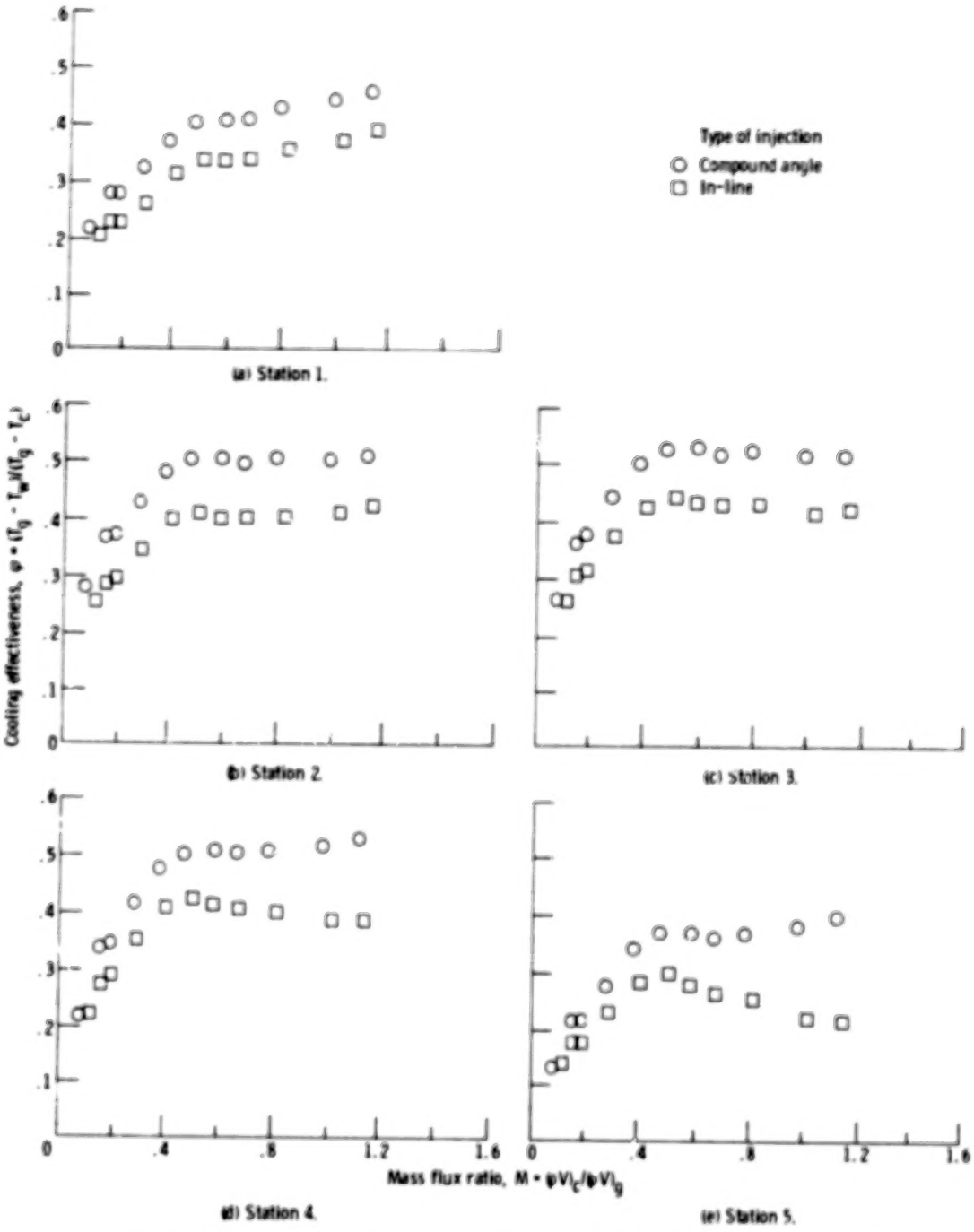

Figure 6. - Cooling effectiveness for film injection from in-line angle holes and compound-angle holes.

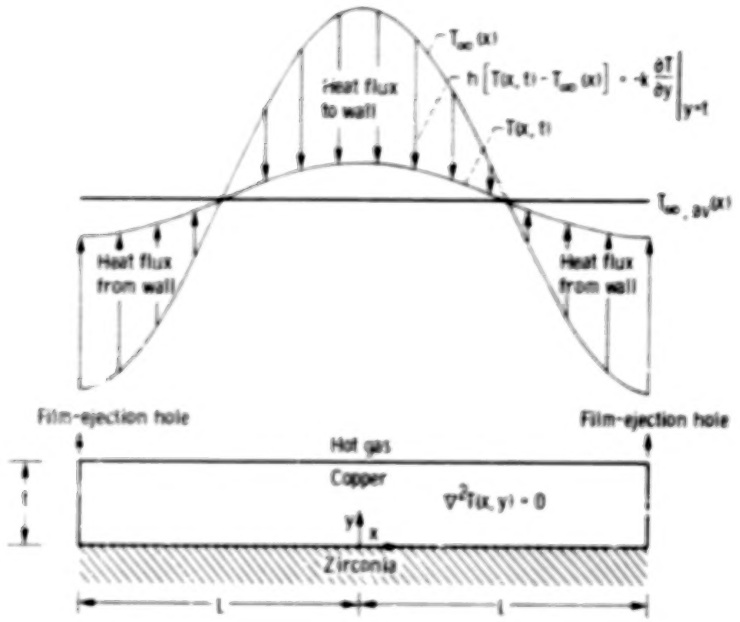

Figure 7. - Coordinate system and heat flux boundary condition for an insulated copper strip inserted into a film cooled wall.

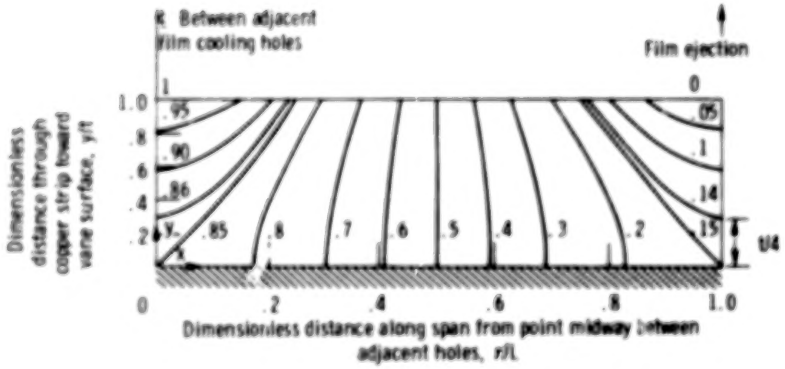

Figure 8 - Dimensionless isotherms within copper strip normalized by hottest and coldest surface temperatures.

1 Report No NASA TP-1095	2 Government Accession No	3 Recipient's Catalog No
4 Title and Subtitle EFFECTS OF FILM INJECTION ANGLE ON TURBINE VANE COOLING		5 Report Date December 1977 6 Performing Organization Code
7 Author(s) James W. Gauntner		8 Performing Organization Report No E-9254 10 Work Unit No 505-04
9 Performing Organization Name and Address National Aeronautics and Space Administration Lewis Research Center Cleveland, Ohio 44135		11 Contract or Grant No 13 Type of Report and Period Covered Technical Paper
12 Sponsoring Agency Name and Address National Aeronautics and Space Administration Washington, D.C. 20546		14 Sponsoring Agency Code
15 Supplementary Notes		

16 Abstract

Film ejection from discrete holes in the suction surface of a turbine vane was studied for hole axes (1) slanted 30° to the surface in the streamwise direction and (2) slanted 30° to the surface and 45° from the streamwise direction toward the hub. The holes were near the throat area in a five-row staggered array with 6-diameter spacing. Mass flux ratios were as high as 1.2. The data were obtained in an annular sector cascade at conditions where both the ratio of the boundary layer momentum thickness-to-hole diameter and the momentum thickness Reynolds number were typical of an advanced turbofan engine at both takeoff and cruise. Wall temperatures were measured downstream of each of the rows of holes. Results of this study are expressed as a comparison of cooling effectiveness between the in-line angle injection and the compound-angle injection as a function of mass flux ratio. These heat transfer results are also compared with the results of a referenced flow visualization study. Also included is a closed-form analytical solution for temperature within the film cooled wall.

17 Key Words (Suggested by Author(s)) Heat transfer Film cooling Turbine blades	18 Distribution Statement Unclassified - unlimited STAR Category 34		
19 Security Classif (of this report) Unclassified	20 Security Classif (of this page) Unclassified	21 No of Pages 23	22 Price* A02

* For sale by the National Technical Information Service, Springfield, Virginia 22161

NASA-Langley, 1977